

Modeling post-shock emergency transfers with the participation of connected-and-autonomous vehicles

Taiyi Zhao^{1,3}, Jingquan Wang^{1*}, Li Sun^{2,3*} & Dina D'Ayala²

1 Key Laboratory of Concrete and Prestressed Concrete Structure of Ministry of Education, School of Civil Engineering, Southeast University, Nanjing, China

2 Department of Civil, Environmental and Geomatic Engineering, University College London, London, United Kingdom

3 These authors contributed equally: Taiyi Zhao, Li Sun

* E-mail: wangjingquan@seu.edu.cn; li.sun@ucl.ac.uk

Abstract: This paper presents a new pathway towards the public health resilience, through the development of a principled understating on the post-hazard emergency transfer of the injured population across densely-populated urban communities, considering the deployment of connected and autonomous vehicles (CAVs). Given the influence on the system resilience of several parameters such as the number and distribution of CAVs, the initial geographic distribution of the injured and the spatiotemporal evolution of the functionality of the integrated hospital-road networks, a multi agent-based modelling (ABM) framework has been established to identify relevant patterns and bottlenecks in injured transfers across hazard-impacted urban communities. In such an ABM framework, each individual vehicle, transferring an injured inhabitant, is modelled as an independent agent, whose traveling is shaped by pre-defined behavioral attributes, while the interplay among those agents is also considered, throughout the entire transfer campaign. Based on a hypothetically catastrophic earthquake scenario, such an ABM framework is employed to model the city-scale, post-shock transfer across Tangshan city, located in one of the most earthquake-prone regions of China. The simulation outcome reveals that the information sharing with regard to the real-time functionality of the local hospital system plays a strategically crucial role, to the avoidance of uncoordinated and prolonged transfers. Furthermore, owing to their capability of intelligent route planning, the participation of CAVs can substantially bolster the rapidity and effectiveness of post-shock transfer campaigns.

Key words: Public health resilience; Post-hazard transfer; Hospital systems; Agent-based model; Connected and autonomous vehicles; Route planning

43 1. Introduction

44 Despite its significant contribution to socio-economic development, the current pace of urbanization
45 poses challenges to the well-being of modern cities, as it is expected that by 2050, 68% of the world
46 population will be urban (United Nations 2018). Increased population density has severe consequence
47 on the vulnerability of the urban infrastructure under disruptive events, such as earthquakes or hurricanes,
48 or pandemics, as emerged in the case of Covid-19 (Civljak et al. 2020, WHO 2022). Given the significant
49 number of injured inhabitants needing life-saving treatments during such disruptive events, timely and
50 sustainable access to the local hospital system plays a strategically crucial role, with regard to the public
51 health resilience of the whole urban community, which the hospital system serves. Nevertheless, the
52 functionality of hospital systems themselves have often proven highly susceptible to disruptions,
53 especially, under damaging earthquakes, **as the lesson learnt from real-world destructive events around**
54 **the globe** (Yavari et al. 2010, Jacques et al. 2014).

55 Such observations have triggered several studies aimed to assess the hospital systems' ability to
56 absorb a significant number of casualties following seismic hazards, and provide a viable pathway
57 towards the continuity of their functionalities. For instance, Cimellaro et al. (2011) presents an
58 organizational model for the response of hospital's emergency department, which enables the estimation
59 of the hospital capacity in real-time, considering the impact of the damage of both structural and non-
60 structural components. In their model, as a straightforward indicator of the time-varying functionality
61 of hospitals, the patient's waiting time has been employed to assess its resilience thereof. In light of the
62 wide range of aspects incorporated, from the configuration to the resources, such a model can serve as
63 an adaptive tool for the risk governance with respect to individual hospitals of interest.

64 More recently, Ceferino et al. (2020) looked into effective response plans of hospital systems under
65 seismic contingencies, and applied their model to Lima city, Peru, under catastrophic earthquake
66 scenarios. Their results demonstrate that the hospital system coordination shall be explored as an
67 effective approach to match demand and supply of the system, and therefore decrease the waiting time
68 of severely-injured patients.

69 Zhai et al. (2021) proposed a comprehensive framework to model the functionality of earthquake-
70 impacted hospitals, which is set to be measured by the ratio of the number of earthquake-induced
71 patients treated to the total number of patients. To that end, a discrete simulation model, which tracks
72 the treatment process of patients, was developed and incorporated into the framework. Such a framework
73 is applied to a general-purpose, secondary hospital in China, and the outcome reveals that the hospital
74 functionality is highly correlated with earthquake intensity measures and highly impacted by damage to
75 nonstructural components and utilities.

76 It shall be highlighted that, apart from the functionality of the individual, or networked hospital

77 systems, the prompt and effective post-shock transfer of injured patients plays an at least equally
78 important role, in terms of the minimization of the death toll, and ultimately, the public health resilience
79 of the earthquake-impacted urban communities.

80 Nonetheless, as repeatedly demonstrated by real-world destructive seismic events, the post-shock
81 transfer of the injured is very likely to be stalled by substantial functionality losses of earthquake-
82 damaged road network embedded in the same urban community (Lin et al. 2010, Hara and Kuwahara
83 2015). Some studies have been carried out to measure the influence of the functionality losses of road
84 networks, which can be even longstanding, on the post-shock emergency evacuation and transfer (Miller
85 and Baker 2016, Toma-Danila et al. 2022). Moreover, potential panic and irrational reactions of the
86 population are also found to play a uniquely crucial role in successful evacuation and transfer, as
87 highlighted by recent studies on the psychological consequences of hazard events, like earthquakes
88 (Cimellaro et al. 2017, Feng et al. 2020, Wang et al. 2021).

89 In parallel, thanks to the latest breakthrough in artificial intelligence-capable machines (Kwiatkowski
90 and Lipson 2019, Schrittwieser et al. 2020), **connected and autonomous vehicles (CAVs)** have been
91 increasingly poised to serve as autonomous transport systems of future urban communities (Lipson and
92 Kurman 2022). Justifiably, large scale deployment and participation of CAVs could also help to
93 revolutionize the post-hazard emergency transfer (Fagnant and Kockelman 2015).

94 Essentially, under earthquake contingencies, compared to human-driven vehicles (HDVs), CAVs can
95 be particularly competitive, in the sense that:

- 96 a. Based on the real-time traffic information, CAVs are capable of planning the travel route
97 autonomously, by resorting to state-of-the-art vehicle-to-infrastructure communication systems
98 (Zhang et al. 2020);
- 99 b. CAVs could be strategically helpful, with regard to the transfer of those earthquake-injured
100 inhabitants (Van den Berg and Verhoef 2016), as well as other vulnerable groups (e.g. those
101 disabled, seniors and children inhabitants, who will be unable or struggling to drive on their own).

102 In view of such a prospect for the amelioration of public health resilience of future urban
103 communities under damaging earthquakes, it is critical to develop a principled understanding on those
104 post-shock transfers with the participation of CAVs, incorporating aspects ranging from the estimation
105 of the casualties and the geographic distribution thereof, to the behavioural pattern of CAVs, and human
106 factors, which has been sparsely studied so far.

107 To fill in such a knowledge gap, an **agent-based model (ABM)** is developed in this paper, to simulate
108 **the post-shock transfer at city scale, incorporating the participation of CAVs. In this ABM, each**
109 **earthquake-injured inhabitant in need of hospitalization is modelled as an individual agent, whose**
110 **behavior is driven by both the hospital choice and the corresponding route planning. The impact of the**
111 **access to real-time information, and the spatiotemporal evolution of the functionality of the integrated**

112 **hospital-road system** on the decision-making of the agents, are examined in-depth in this study,
113 considering **the** hybrid deployment of **CAVs** and **HDVs**.

114 To investigate its **applicability under catastrophic earthquake scenarios**, such an ABM has been
115 employed to model a citywide **post-shock emergency transfer across Tangshan city**, in Hebei province,
116 China, built on a strike-slip active fault, and the site of a catastrophic earthquake of Mw 7.6 in 1976.
117 The simulation outcome reveals that the availability of information about the real-time functionality of
118 the local hospital system plays a decisive role in minimizing transfer and waiting times. Meanwhile,
119 owing to their capability of intelligent route planning, the substantial participation of CAVs can bolster
120 both the rapidity and effectiveness of post-shock transfer campaigns, in a remarkable way.

121 The remainder of this paper includes: Section 2, which highlights the ABM framework; Section 3
122 focuses on the description of the topological configuration of both the hospital and road network
123 embedded in Tangshan city, which serves as **the** application of the framework. **The** geographic
124 distribution of the population across the city as well as the location of **individual hospitals and their**
125 **connectivity are also presented**; Sections 4 and 5 discuss the simulation outcome and draw the
126 corresponding conclusions, respectively.

127

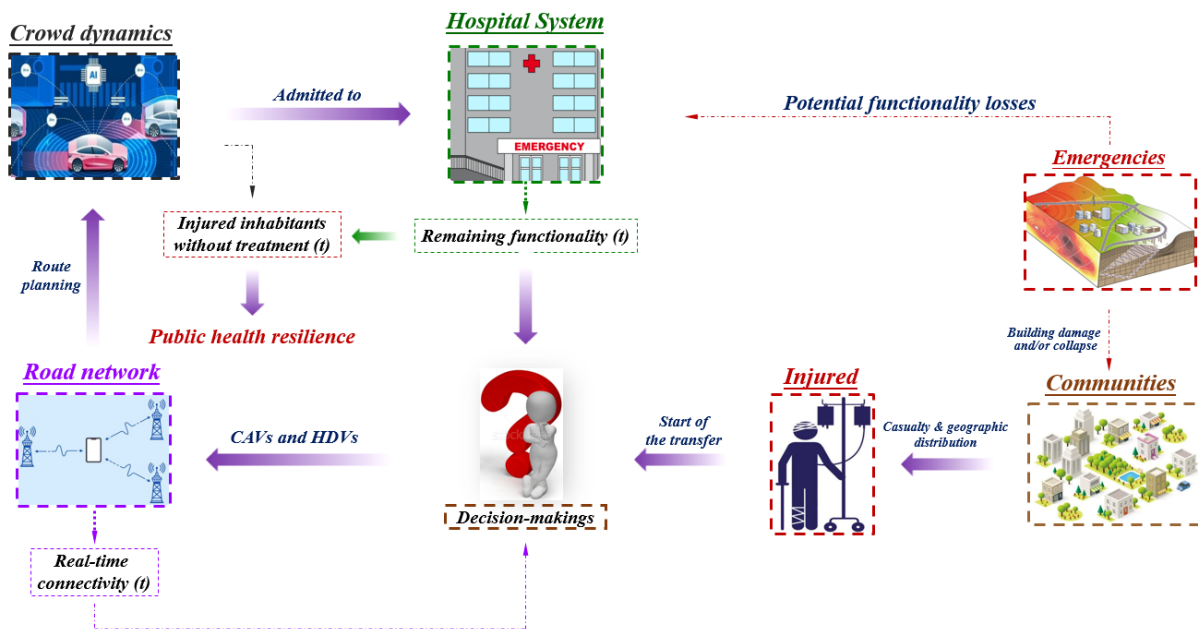
128 **2. Agent-based modeling framework of post-shock emergency transfers**

129 Due to the uncertainty of hazard scenarios, the vulnerability of different infrastructure systems and the
130 interaction among them, as well as the political and economic context, the post-shock emergency
131 transfer across modern urban communities is inherently dynamic and stochastic.

132 As illustrated in Fig. 1, under public emergencies associated with destructive seismic events,
133 significant numbers of injured could be induced by the physical damage and collapse of building
134 structures. Pursuant to the epicenter and magnitude of the earthquake scenario, as well as the location,
135 fragility and occupancy rate of each of those buildings, the level of casualty and the geographic
136 distribution thereof, can be obtained for the whole urban community (Ceferino et al. 2018). For severely-
137 injured inhabitants, it is imperative to transfer them to the closest available hospital to receive life-saving
138 treatments, through either CAVs or HDVs, in an expeditious way. A possible representation of the likely
139 sequence of events relating to injured individuals accessing **emergency department facilities** can be
140 discretised in the following steps: i) selection of a particular hospital, based on **the proximity, the**
141 **reputation and the real-time information regarding the availability of ward beds (if available) of the local**
142 **hospital system**; ii) thereby selection of a travel route, given the connectivity between that selected
143 hospital and the neighbourhood of departure, as well as the **potential connectivity disruption** of the road
144 network following the earthquake (Toma-Danila et al. 2022); iii) as the number of injured increases in
145 the immediate aftermath of the mainshock, crowd dynamics will be generated by the collective motion
146 of individual transfers throughout the post-shock phase (Helbing et al. 2000).

147 Accordingly, the functionality of the hospital system and road network, both of which are essentially
 148 serving as the supply capacity regarding the emergency transfer, is affected by the crowd dynamics,
 149 leading in turn to the reorientation of the decision-making relating to the selection of hospital destination
 150 and travel route, therefore causing the demand to be also temporally and spatially variable and uncertain
 151 (Sun et al. 2015). Justifiably, the adaptivity of the route planning of CAVs, who could shun congested
 152 road segments pursuant to the real-time traffic flow information, will play a strategic role, to the
 153 avoidance of prolonged transfers, which could substantially decrease the mortality rate of earthquake-
 154 impacted communities.

155 To account for the impact of the looped and dynamic interplay between the supply and demand of
 156 the integrated hospital system and road network, an ABM framework has been established in this study,
 157 as a bottom-up and adaptive computational approach to the **post-shock emergency transfers** (Ouyang
 158 2014). In this framework, given the earthquake scenario, the quantity and geographic distribution of the
 159 casualty is assessed in the absorption phase (Ouyang et al. 2012), while the mass transfer is modelled in
 160 the corresponding phase of the immediate aftermath of earthquakes, where each of the vehicle (either
 161 CAVs or HDVs) participating in the transfer will be modelled as an intelligent agent (Sun et al. 2021).
 162 The trajectory of the emergency transfer throughout the whole seismic event can be thereby tracked, the
 163 rapidity and effectiveness of which will serve as a measure on the public health resilience of the whole
 164 community.



165
 166 Fig. 1. Post-shock emergency transfer across the earthquake-impacted community-hospital system-road network.
 167

168 **2.1. Earthquake hazard and casualty model**

169 In this framework, to assess the number and distribution of the earthquake-injured inhabitants, damage
 170 behaviour of each of building structures across the whole urban community is modelled by its fragility

171 and the corresponding intensity measures, which are usually determined by ground motion attenuation
172 models and the given earthquake scenario (Stupazzini et al. 2021). In this study, without loss of
173 generality, the attenuation model developed by Atkinson and Boore (1995), applicable to earthquakes
174 with $4 \leq M_w \leq 7.25$, is incorporated into the framework, to enable the study of post-shock emergency
175 transfer under earthquake scenarios with high magnitude, whereby trivial simulation outcomes can be
176 avoided.

177 Mathematically, the peak ground acceleration, which is the intensity measure employed in this study,
178 is therefore obtained following Eq. (1):

$$179 \quad \log(PGA) = a_1 + a_2(M_w - 6) + a_3(M_w - 6)^2 - \log R_e - a_4 R_e \quad (1)$$

180 Here, M_w and R_e refers to the earthquake magnitude and the corresponding epicentral distance,
181 respectively; Meanwhile, the value of the parameters a_1 , a_2 , a_3 and a_4 are set to be 3.79, 0.298, -0.0536
182 and 0.00135, respectively, as obtained from regression analysis (Atkinson and Boore 1995). Alternative
183 attenuation laws specific to the site of interest or intensity measures, suitable to identify the response of
184 specific structural typologies, can be equally employed in the framework.

185 A thorough review of casualty estimation methods has been provided recently by Yan et al (2021).
186 Models can be empirical (based on past data) or predictive (based on causal factors, such as buildings'
187 vulnerability) and be applicable at different scales, from regional to local. In the present study, given the
188 damage state of each individual building determined through fragility analysis based on the peak ground
189 acceleration at its site, the community-level casualty analysis can be run following the model proposed
190 by Coburn et al. (1992), which accounts for the occupancy rate of buildings and the total population of
191 the community. It is noteworthy that, in this study, only those inhabitants sustaining the hospitalization-
192 level injury are assumed to participate in the post-shock emergency transfer, whereby the city-wide
193 simulation can be more tractable.

194 Besides, in view of the spatial-temporal variability of the population across modern urban
195 communities driven by their modus operandi, the impact of different timing of earthquake hazards on
196 the post-shock transfer is also considered in this study (Ceferino et al. 2020). Specifically, a daytime and
197 a nighttime scenario, respectively, will be considered. They are simulated by considering that the
198 majority of the inhabitants are located in the downtown area of the community of interest, during
199 daytime, while during nighttime the majority will be in residential neighborhoods, which are often
200 located at the periphery of modern communities.

201

202 **2.2. Hospital selection criteria**

203 Let $C = \{n_1, n_2, \dots, n_m\}$ denote the array of neighborhoods embedded in the urban community of interest,
204 where m is the total number of those neighborhoods. Meanwhile, $HS = \{h_1, h_2, \dots, h_k\}$ stands for the

205 local hospital system consisting of k individual hospitals. In this research, for hospital h_i ($i \in k$) in the
 206 HS , its functionality will be characterized by two attributes, denoted as C_i^{max} , and $IA_i(t)$, respectively.
 207 As a constant, C_i^{max} stands for the maximum healthcare capacity of h_i , while $IA_i(t)$ refers to the
 208 number of the injured, who **have already been admitted** to this hospital, at time point t . Its remaining
 209 healthcare capacity at such a moment, denoted as $RC_i(t)$, can be therefore obtained following Eq. (2):

$$210 \quad RC_i(t) = \begin{cases} C_i^{max} - IA_i(t), & IA_i(t) < C_i^{max} \\ 0, & IA_i(t) = C_i^{max} \end{cases} \quad (2)$$

211 Equation 2 shows that any injured patient arriving at h_i at a time t^+ greater than time $t=T_0$, when
 212 $RC_i(T_0)=0$, will need to re-select among the remaining hospitals with spare capacity to receive medical
 213 treatments. By doing so, the heterogeneity (e.g. regarding the functionality) of modern hospital systems
 214 can be taken into account, by the proposed ABM framework. This condition arises from the assumption,
 215 legitimate in the timeframe of this simulation, that no patient will be discharged during the period of
 216 time needed to deliver all casualties to an emergency department unit.

217 In the pre-shock phase, apart from those centralized transfer strategies (Ceferino et al. 2020), the
 218 hospital selection of individual inhabitants will be collectively driven by a host of influential factors,
 219 ranging from the reputation of every single hospital, to the personal preference and household financial
 220 conditions (Hassan and Mahmoud 2020), and is thus fairly complex unregulated phenomenon. In the
 221 immediate aftermath of an earthquake, however, given the type of injuries usually sustained, the travel
 222 time needed to reach a given hospital, also plays a decisive role in the selection of the destination (Del
 223 Papa et al. 2019). Clearly, the shorter the travel time is, the more likely those severely-injured can access
 224 life-saving treatments, and thereby survive.

225 As an endeavor to balance the trade-off between the inclusiveness and computational tractability, the
 226 hospital selection of injured inhabitants in neighborhood n_j ($j \in m$) will be following the criterion
 227 formulated in Eq. (3):

$$228 \quad P_{i,j} = \frac{RC_i(t) \varpi D_{i,j}^{-\xi}}{\sum_{i=1}^k RC_i(t) \varpi D_{i,j}^{-\xi}} \quad (3)$$

229 whereby, $D_{i,j}$ stands for the length of the shortest path between that neighborhood and hospital h_i , which
 230 is obtained using the classical Dijkstra algorithm (Dijkstra 1959). The attraction coefficient, denoted as
 231 ϖ , is introduced to serve as a measure on how decisive the remaining healthcare capacity of one
 232 particular hospital is, with regard to **the selection of the destination**: the higher the ϖ value, the more
 233 likely hospitals with greater remaining capacity are chosen. Similarly, the resistance coefficient, denoted
 234 as ξ , is employed to measure the effect of the travel distance on destination decision-making.
 235 Mathematically, for each hospital, their distance to the neighborhood of interest will be increasingly
 236 disproportionate to the likelihood of being picked by the inhabitants living there, in the case of higher ξ
 237 values (Wu et al. 2010).

238 It is noteworthy that, in this study, it is also assumed that the decision-making of the injured
 239 inhabitants, who are modelled as the autonomous agents in the ABM framework, **will be independent**
 240 from others. Besides, to avoid unaffordable computational costs, throughout the post-shock emergency
 241 transfer, once the decision is made, the re-selection of the targeted hospital en route will not be
 242 considered in the following case-study, until the arrival at the selected one (Wang et al. 2016). If, upon
 243 arrival, the selected hospital capacity is saturated, they will then need to re-select their new destination,
 244 according to Eq. (3).

245 Furthermore, it shall be highlighted that, the hospital selection following Eq. (3) is conditioned upon
 246 the enduring information sharing, which may not hold true, with respect to damaging earthquakes.
 247 Regarding those cases, the agents will select the hospital based upon the pre-shock functionality level,
 248 namely, replace $RC_i(t)$ with C_i^{max} , in Eq. (3).

249

250 **2.3. Travel route planning of CAVs**

251 Inhabitants engaging in post-hazard evacuations and transfers would often resort to various ways of
 252 travel (Li et al. 2020). Nonetheless, given the urgency of the rescue in the wake of damaging earthquakes,
 253 all the injured inhabitants participating in the post-shock transfer are assumed to be transferred to the
 254 local hospital system by vehicles (not by walking), in this study. **Without losses of generality**, it is
 255 assumed that agents driving HDVs are experience-based, who will always choose the shortest path to
 256 the targeted hospital, as obtained through the topology of the local road network, regardless of the real-
 257 time traffic flow en route. By comparison, CAVs are assumed to be able to reorient their path through
 258 dynamic planning, in the course of post-shock transfers.

259 Mathematically, dynamic planning is a general paradigm, which can be employed to fulfil the
 260 optimization objective, with respect to sequential decision-makings (Russell and Norvig 2021).
 261 Regarding CAVs participating in post-shock transfers, the objective is the minimization of the expected
 262 travel time (ETT). Pursuant to that objective, as shown in Fig. 2, for a CAV agent (who is departing from
 263 the neighborhood n_j and has picked the hospital h_i) at the l^{th} decision-moment (referred to as DM_l) en
 264 route, i.e. the l^{th} crossroad it has arrived at, the action to be taken (namely, which particular road segment
 265 it will then switch to), denoted as A_l , is determined by Eq. (4):

$$266 \quad A_l = \arg \min_p ETT(TR(V, A), TF(DM_l), a_p) \quad (p=1, 2, \dots, Q) \quad (4)$$

267 Here, $TR(V, A)$ is the topological model of the local road network established based on graph theory,
 268 where $V = \{v_1, v_2, \dots, v_R\}$ is the set of R vertices of the network, which stand for the crossroads,
 269 neighborhoods and hospitals, respectively. Meanwhile, $A = \{a_1, a_2, \dots, a_T\}$ refers to the corresponding T
 270 arcs, namely, the road segments. Among those arcs, a_p ($p=1, 2, \dots, Q$) stand for the array of those Q arcs
 271 connected to the l^{th} crossroad where the agent is now, excluding the one, which the agent has just

272 travelled along (whereby infinite loops can be avoided). In particular, to consider the impact of the real-
 273 time traffic flow across the whole road network, referred to as $TF(DM_l)$, on the adaptive decision-
 274 makings of CAV agents, the classic impedance function has been introduced into this framework
 275 (Branston 1976), and the ETT needed regarding road segment a_p (denoted as $ET_p(DM_l)$) is therefore
 276 obtained by Eq. (5):

$$277 \quad ET_p(DM_l) = FT_p \left(1 + \alpha \left[\frac{TF_p(DM_l)}{MT_p} \right]^\beta \right) \quad (5)$$

278 Here, FT_p denotes the free travel time of a_p that can be determined by L_a/v_c , where L_a stands for
 279 the length of this arc, while v_c refers to the free flow travel speed of the CAV. Meanwhile, $TF_p(DM_l)$
 280 and MT_p denote the real-time traffic flow of a_p at the moment DM_l , and the maximum traffic-carrying
 281 capacity of such a road segment, respectively. Moreover, the values of the parameters α and β have been
 282 set to be 4.5 and 4.0, respectively, in this research (Feng et al. 2020).

283 As shown in Fig. 2, driven by the dynamic programming and the choice of a_p , the CAV agent will
 284 virtually reach the next crossroad v_l^p , after a period of time $ET_p(DM_l)$. To minimize the total expected
 285 travel time of the transfer, the agent can, at this point, choose a route (among all the possible ones,
 286 pursuant to the choice of a_p) associated with the minimum travel time needed thereafter to arrive at the
 287 hospital h_i from v_l^p (Hart et al. 1968). For any particular route R_g ($g = 1, 2, \dots, NR_l^p$), the corresponding
 288 time span, denoted as $TT(R_g)$, can be thereby determined through Eq. (6):

$$289 \quad TT(R_g) = \sum_{s=1}^{N_p^g} FT_s \left(1 + \alpha \left[\frac{RT_s(DM_l)}{MT_s} \right]^\beta \right) \quad (6)$$

290 Here, N_p^g stands for the total number of road segments that route comprises. Therefore,
 291 $ETT(TR(V, A), TF(DM_l), a_p)$ can be obtained by Eq. (7):

$$292 \quad ETT(TR(V, A), TF(DM_l), a_p) = ET_p(DM_l) + \min(TT(R_g)), g = 1, 2, \dots, NR_l^p \quad (7)$$

293 As illustrated in Fig. 2, after the execution of the action A_l , the CAV agent will travel along the
 294 corresponding road segment, until the arrival of the next crossroad, namely, the $(l+1)^{th}$ one. The decision
 295 at such a moment, DM_{l+1} , will be made following the same dynamic programming procedure described
 296 above. Such an iteration will continue, until the agent has reached hospital h_i eventually.

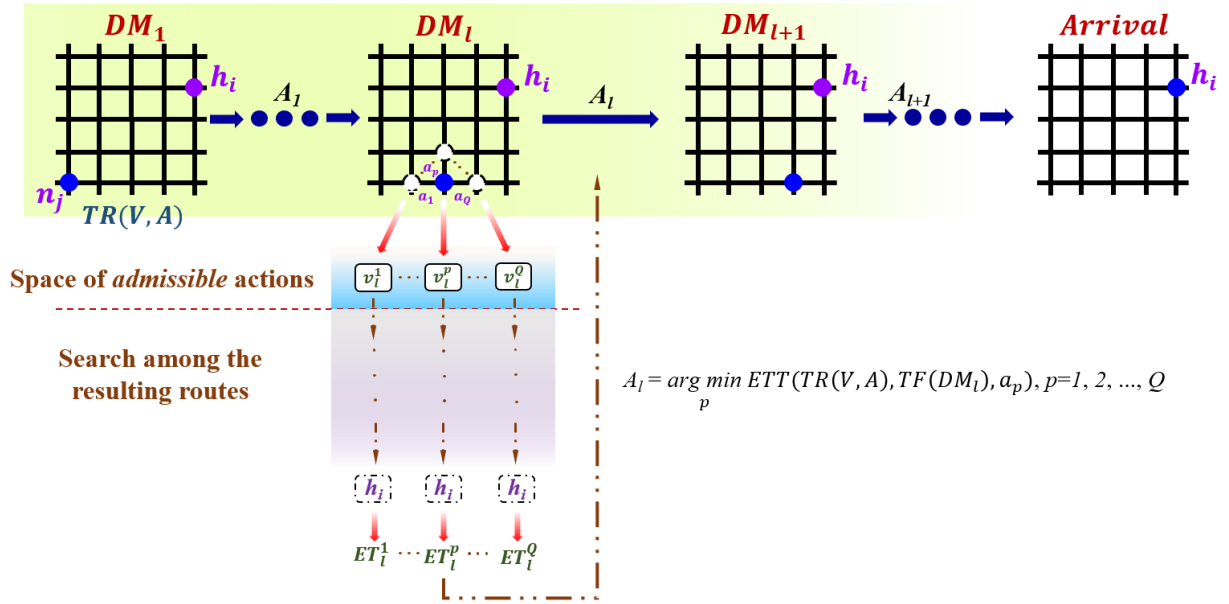


Fig. 2. Dynamic route planning of CAV agents.

297

298

299

300

2.4. Traffic dynamic model on the system-level

301

Despite the straightforward pattern of the individual agent's behavior presented above, it can be fairly challenging to model the dynamic, self-organized traffic flow across city-scale road networks (Helbing and Mazloumian 2009) on the system-level, when compounded by earthquake post-shock damage, in view of the potentially prolonged traffic congestion, as well as the panic and irrationality of considerable quantity of individual drivers (Feng et al. 2020). To ensure the tractability of the simulation, a queuing model (Cetin et al. 2003) has been integrated into the ABM framework, whereby the traffic dynamics regarding the mass crowd consisting of both CAVs and HDVs can be shaped. Following such a model, when an agent who is driving either a CAV or HDV has reached a crossroad, it can switch to the next road segment, only if the following requirements have all been fulfilled:

310

- (1) Given a set flow limit for each road segment, the number of vehicles that can switch at every time step cannot exceed that limit;
- (2) The remaining space of the targeted road segment can still allow for additional vehicles;
- (3) In case of multiple vehicles being ready to switch at the same time, the one which has reached the crossroad first will also be allowed to go first.

314

315

316

2.5. Performance of post-shock emergency transfers

317

To gauge their performance at system-level, the gross transfer time (GTT) has been proposed as the measure on the city-scale transfers, and can be quantified by Eq. (8):

318

319

$$GTT = \sum_{v=1}^{N_w} DT_v \quad (8)$$

320

where N_w is the total number of injured people, who are engaging in the post-shock transfer, under any particular earthquake scenario. Meanwhile, DT_v denotes the total travel time from its origin to the

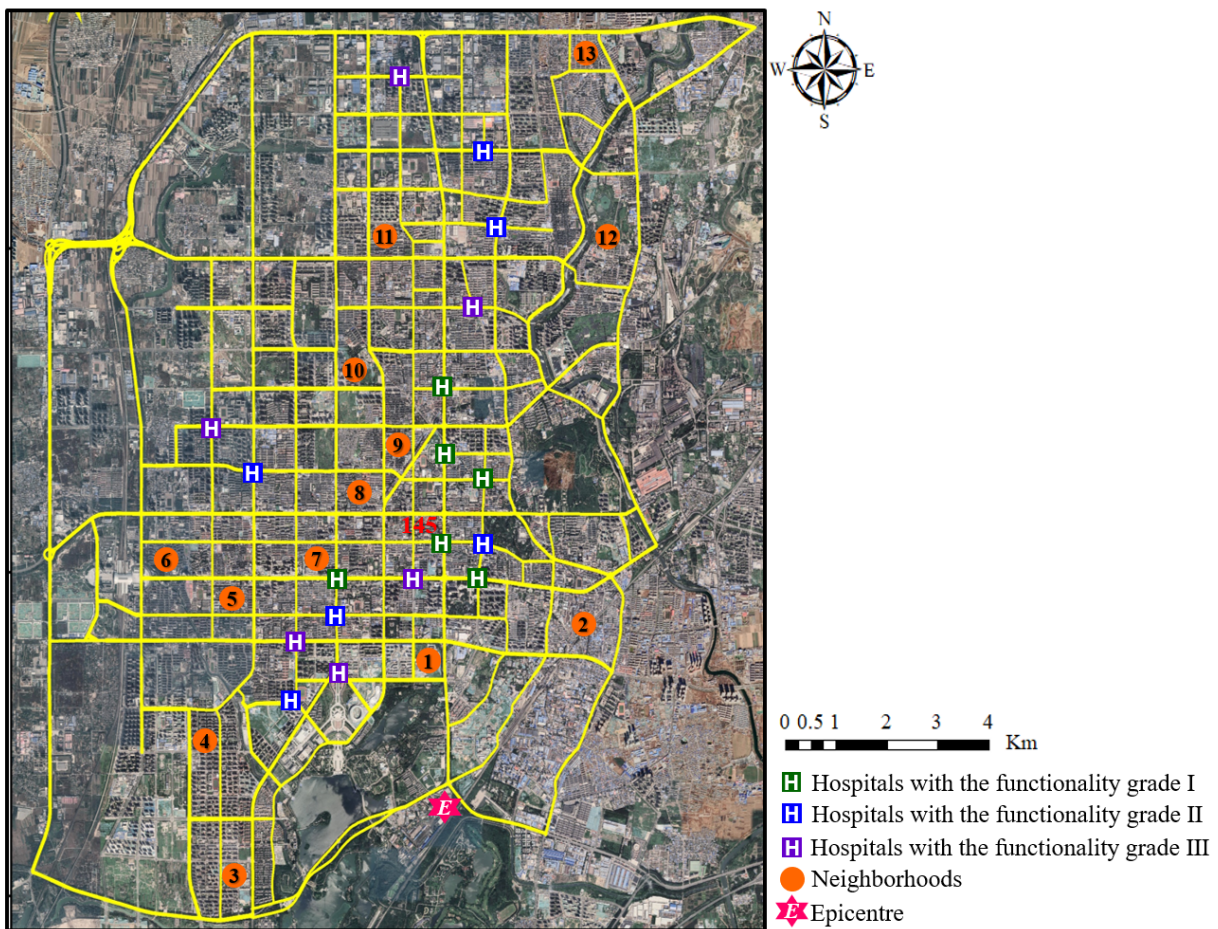
321

322 hospital of the agent v . Besides, it is also noteworthy that, in this framework, such a duration does not
323 include the hospital services' waiting time, upon arrival. Additionally, once admitted to, the discharge
324 of those injured inhabitants from hospitals will not be modelled neither in this study, given the time scale
325 of the immediate aftermath of hazard events.
326

327 3. Case study

328 3.1. Topology and operational conditions of the hospital system-road network

329 To examine its applicability, the ABM framework developed in Section 2 has been applied to the
330 integrated hospital system-road network of Tangshan city, which is an industrial hub located in one of
331 the most earthquake-prone regions of China (He et al. 2016), and a corresponding case study was
332 conducted under hypothetical, damaging earthquake scenarios. The simplified topology of such a
333 networked hospital system-road network-community is plotted in Fig. 3. For each of the neighborhood
334 across the whole network, without losses of generality, it is assumed that the reinforced concrete and
335 masonry structures will account for 50% of the gross number of buildings, respectively. Besides, the
336 fragility model proposed by Jaiswal et al. (2011) is employed to shape the seismic response of these two
337 different types of structures.



339
340

Fig. 3. Topology of the integrated hospital system-road network-community.

341 Specifically, the road network consists of 216 vertices and 375 arcs. Meanwhile, 18 hospitals with
342 different functionality grades have been incorporated into the hospital system. As shown in Table 1, a
343 total of three functionality grades, measured by the quantity of ward beds, are considered in this study
344 (Li et al. 2008). Besides, each of those grades has been assigned to 6 hospitals, so that the total number
345 of beds coincides with the number of injured (see Table 1 and Fig. 3).

346

Table 1. Information of the hospital system

Functionality grades	Corresponding nodes						Number of ward beds
<i>I</i>	94	117	130	145	155	159	2,400
<i>II</i>	32	57	112	146	168	203	1,200
<i>III</i>	13	76	99	157	180	193	680
Total							25,680

347

348 In parallel, the corresponding urban community includes 13 neighborhoods, whose population is
349 summarized in Table 2, leading to a total of 702,394 inhabitants residing in the whole area. For each of
350 those neighborhoods, its population are assumed to be equally distributed on those nodes associated
351 with it.

352

Table 2. Information of the neighborhoods of the community

Number	Neighborhood	Corresponding nodes						Population
1	Guang Chang	1	184	195	196			42,771
2	Yong Hong Qiao	1	161	186	187			21,743
3	Liang Jia Tun	2	208	213	214			62,691
4	Hui Min Dao	1	190	199	200			70,391
5	You Yi	1	153	165	166			41,486
6	Guo Yuan Zhen	1	122	138	139			64,715
7	Da Li	1	125	141	142			66,001
8	Xiang Yun Dao	1	126	127			14,460	
9	Wen Hua Lu	1	104	116			66,677	
10	Ji Chang Lu	8	83	92	93			68,201
11	Gao Xin Qu	4	41	54	55	59	60	100,002
12	Long Dong	4	46	63	72	73		44,426
13	He Bei Lu	7	8	16	17			38,830

353

354 3.2. Scenario-based simulation following the ABM framework

355 In view of the significant uncertainty associated with seismic hazards, the behavioral pattern (regarding

356 the hospital selection, as well as the route planning) of individual injured inhabitants, as well as the
 357 number of available CAVs, following the ABM framework described above, Monte Carlo simulations
 358 are run to consider their collective impact on the city-scale, post-shock transfers. For both the CAV and
 359 HDV, their travelling speed are set to be 4m/s in this study, to consider the potential influence of debris,
 360 etc., throughout seismic events.

361 Meanwhile, given the expensive computational cost, 50 Monte Carlo simulations are run for each
 362 single scenario included in this case study, which have been listed in Table 3.

363 Table 3. Setup of scenarios included in the case-study

Scenario	Information accessibility of each single hospital	Timing of earthquakes
1	yes	daytime
2	no	daytime
3	yes	nighttime
4	no	nighttime

364
 365 Specifically, in light of the modus operandi of most modern urban communities, the majority of their
 366 inhabitants are expected to be either working, studying, or shopping across downtown areas, in the
 367 daytime. Conversely, they are supposed to be resting or sleeping at home, usually located on the outskirts
 368 of the city, at nighttime. Therefore, the timing of the mainshock of **destructive earthquakes** is expected
 369 to have a nonnegligible impact on the post-shock transfer, given that distinct spatial distribution of
 370 populations. Accordingly, two different scenarios, where earthquake is occurring at daytime and
 371 nighttime, respectively, have been considered in this research. **In the first case**, 80% of the population
 372 affiliated to neighborhoods with ID Nos. 2, 3, 4, 11, 12, and 13 are assumed to relocate to neighborhoods
 373 with ID Nos. 1, 5, 6, 7, 8, 9, and 10 (Fig. 3). On the contrary, in terms of nighttime, the converse applies.
 374 The distribution of the injured population for the two cases is detailed in Table 4.

375 Table 4. Distribution of injured inhabitants under the scenario with earthquake at daytime and nighttime

Number	Neighborhood	Daytime	Nighttime
1	Guang Chang	3,071	437
2	Yong Hong Qiao	223	2,857
3	Liang Jia Tun	545	3,971
4	Hui Min Dao	551	4,487
5	You Yi	3,738	312
6	Guo Yuan Zhen	4,369	433
7	Da Li	4,157	514
8	Xiang Yun Dao	1,715	115
9	Wen Hua Lu	3,132	497
10	Ji Chang Lu	3,134	467

11	Gao Xin Qu	585	5,283
12	Long Dong	269	3,932
13	He Bei Lu	191	2,375

376

377 **It is also noteworthy that**, real-world earthquake events have demonstrated that modern
 378 telecommunication systems can also be seismically-vulnerable, and thus sustain earthquake-initiated
 379 functionality losses (Krishnamurthy et al. 2016), whereby the information sharing regarding the real-
 380 time functionality status of the local hospital system can be substantially disrupted, throughout post-
 381 shock emergency transfers. Therefore, for each of the two scenarios described above, the cases where
 382 the real-time information is, and is not available, respectively, will be further introduced. Hence, a total
 383 of four different scenarios have been generated for this case study, as shown in Table 3. Moreover, for
 384 each of those scenarios, different proportions of CAVs participating in the post-shock emergency
 385 transfer are accounted for by considering five cases, from 20% to 100% in increments of 20%.

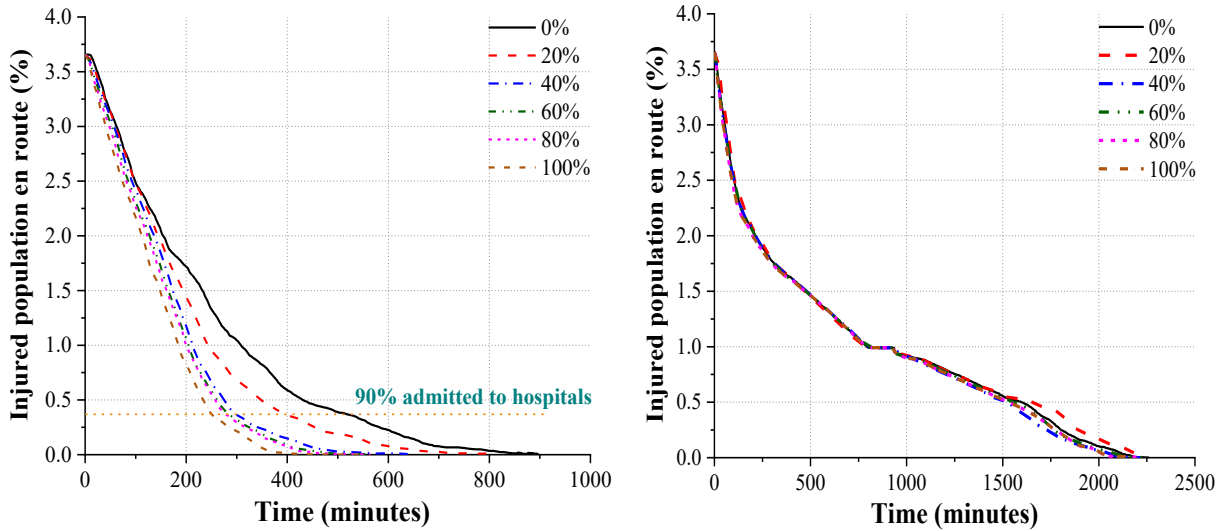
386 Finally, to generate nontrivial and realistic simulation outcome, one particular earthquake scenario
 387 with the magnitude of 7.25 and epicentral depth of 10 km are considered in this paper, which is consistent
 388 with the real-world, historical seismic activities recorded across Tangshan city (Lomnitz and Lomnitz
 389 1978, Chen et al. 2021).

390

391 **4. Simulation results**

392 ***4.1. Daytime Scenario***

393 Figure 4 tracks the median percentage of the injured population en route (IPER) to hospitals versus the
 394 gross population in the region, throughout the post-shock emergency transfer, under the daytime
 395 scenario. In particular, the results associated with the corresponding cases with and without the real-
 396 time information sharing, regarding the functionality status of the local hospital system (which is
 397 measured by the amount of the remaining ward beds, as described in Section 2) have been plotted in
 398 Figs. 4(a) and 4(b), respectively.



(a) With information sharing (b) Without information sharing
 Fig. 4. Median percentage of injured population en route under daytime scenario.

399
 400
 401
 402

403 As shown in Fig. 4, the number of injured in need of hospitalization is found to reach 25,680, which
 404 account for 3.656% of the total population, under such a catastrophic earthquake scenario. From Fig.
 405 4(a), notably, the post-shock emergency transfer is demonstrated to be going more smoothly and
 406 promptly, when more CAVs are engaged in the campaign. Quantitatively, in terms of the two extreme
 407 cases (with 0 and 100% CAVs, respectively), the corresponding GTT (obtained following Eq. (8)) of the
 408 whole transfer campaign are found to be approximately 15 and 9.1 hours, respectively, signaling a 39%
 409 reduction, owing to the presence of CAVs. In particular, it can be further found from the trajectory
 410 associated with the case with 100% CAVs that, the IPER value is decreasing with an almost-constant
 411 slope until the 250th minutes after the shock, when 90% of the injured have been delivered to hospitals.
 412 By comparison, in the case without any CAV, its trajectory reveals that the transfer is becoming slower
 413 after 50% of the injured are delivered to the local hospital system, and it takes 520 minutes, that is 2.08
 414 times longer (than that associated with the case with 100% CAVs), for the 90% to be transferred.
 415 Justifiably, such a significant reduction of GTT is strategically crucial to the minimization of the fatality
 416 rate, as well as socio-economic losses of earthquake-impacted urban communities.

417 Table 5. Median GTT with regard to different percentage of CAV agents under daytime scenario

Scenarios considered	GTT (minutes)					
	0%	20%	40%	60%	80%	100%
scenario 1 (with)	900	805	641	561	567	547
scenario 2 (without)	2,261	2,247	2,217	2,224	2,208	2,191

418
 419
 420

Nonetheless, it shall be also highlighted that the resulting GTT is not decreasing linearly with the growing percentage of CAVs participating in the transfer campaigns. From Fig. 4(a), shows a step

421 change in the delivery when the proportion of CAVs reach 40%. As shown in Table 5, the resulting GTT
422 in such a case is 10.7 hours, 28.7% shorter than that regarding the baseline. On the other hand, the time
423 reduction for higher proportions of CAVs is not really significant. Such an observation suggests that,
424 given their autonomous decision-making capabilities under public emergencies, the deployment of a
425 fleet of CAVs, **even just on a moderate scale**, can be leveraged as an effective tool to ameliorate public
426 health resilience of future urban communities imperiled by natural hazards.

427 Moreover, the contribution of CAVs to public health resilience appear significantly diminished, when
428 the real-time information regarding hospital system functionality is inaccessible, as shown in Fig. 4(b).
429 Although the slope is initially steeper than the case with information, the baseline GTT is more than
430 doubled. Overall, the trajectories associated with all the different cases are overlapping, throughout the
431 entirety of the post-shock transfer. Quantitatively, even for the case of 100% CAVs, the resulting GTT
432 reaches 36.5 hours, merely 3.1% lower than that of the baseline, signaling an almost-negligible
433 contribution of CAVs on the post-shock transfer. Such a stark contrast between scenarios 1 and 2 reveals
434 that the contribution of CAVs can be maximized, only when real-time information about **the hospital**
435 **capacity** is continually available. Hence, it further suggests that the interdependence among different
436 critical infrastructure systems should be accounted for, in terms of the risk governance and public health
437 resilience amelioration of future urban communities.

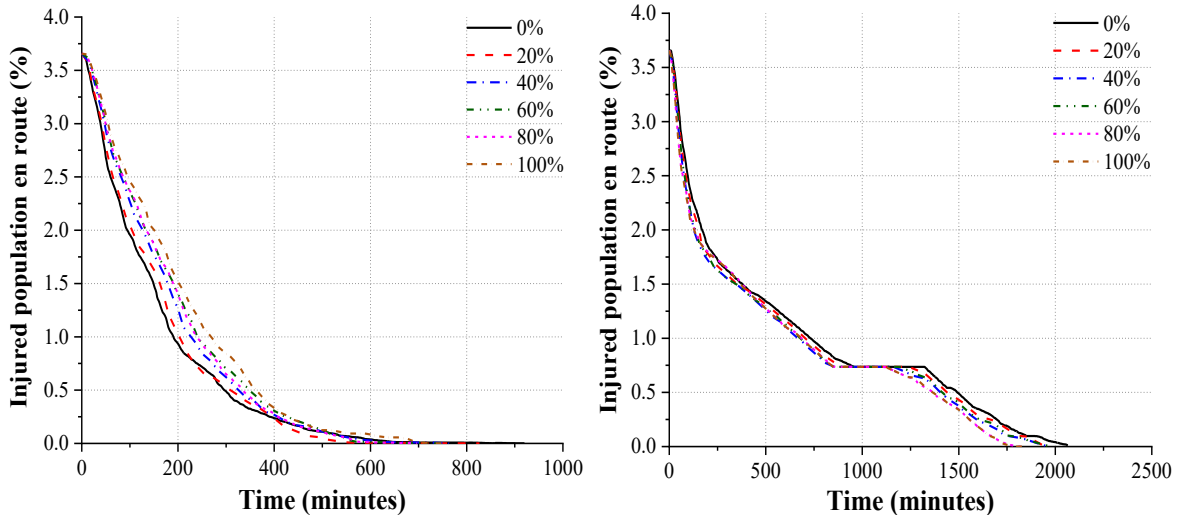
438 In parallel, as shown in Table 5, it can be found that, regarding the cases with 0% and 100% CAVs,
439 for scenario 2, the obtained GTT is 2.5 and 4 time longer than the corresponding values associated with
440 scenario 1, respectively. It therefore reveals that, due to the lack of real-time information, substantially
441 more injured inhabitants will be delivered to hospitals with initially higher functionality grade, which
442 can be thus overwhelmed, given such a significant healthcare demand, in the wake of damaging
443 earthquakes. As a result, considerable fraction of those wounded will then need to re-select, leading to
444 a much longer transfer campaign. This is identified in Fig. 4(b) by the portion of the GTT curve with
445 horizontal tangent.

446 447 **4.2. Nighttime Scenario**

448 For the nighttime scenarios, a larger proportion of the injured are distributed across neighborhoods with
449 the ID Nos. 2, 3, 4, 11, 12, and 13, whereas most of the hospitals are located across the downtown area
450 (Fig. 3). The corresponding post-shock transfer is thus expected to be more time-consuming, given the
451 longer distance to the local hospital system, and likely to be hindered by the limited choice of alternative
452 routes to the hospital and therefore the possibility of hold ups for many of the injured.

453 As shown in Table 6, unlike the earthquake at daytime, for both scenarios 3 and 4, the resulting GTTs
454 are not found to be decreasing monotonically, given the increasing percentage of CAVs. Specifically,
455 the GTT reaches the minimum, when the percentage of CAVs is **set to be 80%** for both scenarios, leading

456 to a reduction by 24.2% (11.6 hours versus 15.3 hours) and 11.7% (30.4 hours versus 34.4 hours),
 457 respectively, highlighting again that the lack of information sharing will reduce the effect of CAVs.



458
 459 (a) With information sharing
 460 (b) Without information sharing
 Fig. 5. Median percentage of injured population en route under nighttime scenario.

461 In particular, Fig. 5(a) reveals that, without the participation of any CAV, the IPER reduces more
 462 quickly in the earlier stage, compared to other cases. Such a significant difference from the results shown
 463 in Fig. 4(a) shows that, as the simulation starts with the road network without any traffic flow, the
 464 transfer is initially more efficient when the injured choose the shortest path, rather than the input
 465 provided by dynamic route programming. However, the transfer becomes increasingly slow in the latter
 466 stage, when a relatively small proportion of agents are engaging in the re-direction and new destination
 467 as the treatment in the targeted hospital is inaccessible on arrival, and they are required to travel among
 468 different hospitals, across the crowded downtown area. Nevertheless, owing to their adaptivity, all the
 469 other cases with CVAs catch up and outpace the baseline, even though both the reduction in time and
 470 the percentage of injured involved are rather marginal.

471 The impact of the hospital re-selection is more clearly pronounced, for the post-shock transfer under
 472 scenario 4, as shown in Fig. 5(b). It can be found that, until 80% of the injured have reached the local
 473 hospital system, the trajectories associated with all the different cases are nearly identical, suggesting a
 474 fairly marginal contribution of the increasing amount of CAVs, which is similar to the pattern found
 475 from Fig. 4(b).

476 Table 6. Median GTT with regard to different percentage of CAV agents under nighttime scenario

Scenarios considered	GTT (minutes)					
	0%	20%	40%	60%	80%	100%
scenario 3 (with)	919	828	765	759	697	756
scenario 4 (without)	2,066	1,948	1,949	1,966	1,824	1,836

477 However, regarding the baseline case, a long plateau is observed thereafter, indicating that a

478 significant fraction of the injured population, who are travelling along the shortest path to the re-selected
479 hospital, without exploring the connectivity of the other road segments of the road network, are stuck in
480 traffic jam. By comparison, as more CAVs are deployed, the length of the plateau shortens, although the
481 slope remains similar among the different cases.

482

483 **4.3. Discussions**

484 In Sections 4.1 and 4.2, the obtained simulation outcome regarding the 4 different scenarios have
485 highlighted the complexity of the post-shock transfer of **large number** of injured inhabitants across
486 modern urban communities, as a combined result of different earthquake scenarios, the functionality
487 supply capacity of the local hospital system, the topological configuration of the corresponding road
488 network, as well as the crowd dynamics collectively driven by the behavioral pattern of each individual
489 agents engaging in the transfer campaign. Against this backdrop, this Section attempts to dig further into
490 the result, and generate new insights that can be generalizable to other urban communities with different
491 scales and infrastructures systems with different functionality capacities and topologies.

492 Quantitatively, among all the cases considered in Sections 4.1 and 4.2, the one with 100% CAVs
493 under scenario 1 has been found to lead to the minimum GTT of the whole transfer campaign, although
494 similar results can be obtained by engaging only 60% of CAVs. As described above, according to the
495 setup of such a case, most of the injured inhabitants will be in the downtown area, where a concentrated
496 functionality demand on the hospital system has been thus generated. Meanwhile, it can be found from
497 Fig. 3 that, all those hospitals with the functionality grade *I* are also embedded in such an area (which is
498 indeed fairly common, with regard to the configuration of the majority of modern urban communities),
499 leading to a better match between the local functionality supply and demand, whereby the re-selection
500 and re-transfer can be largely avoided. In addition, it shall be highlighted that the redundancy of the
501 local road network topology is indeed playing an equally decisive role to the effective transfer, in the
502 sense that all the hospitals in such an area are well-connected, and thereby much more accessible from
503 different neighborhoods nearby, especially, when considerable number of CVAs, which benefit from the
504 real-time connectivity of the whole road network, are participating in the transfer. For example, as shown
505 in Fig. 3, the hospital at node 145 is not only close to all those neighborhoods with ID Nos. 1, 5, 6, 7, 8,
506 9, and 10, but is also reachable by up to a total of four different road segments. By comparison, the
507 hospital system is considerably sparser in the peripheral neighborhoods. In addition, the topology of the
508 road network in those areas is also significantly less redundant, which indicates that hospitals can be
509 also less accessible in such areas (Byun and D' Ayala 2022). As a result, traffic congestion is thus more
510 likely to be triggered in the course of the emergency transfer, especially, when all the agents choose to
511 travel by adhering to the shortest path to those hospitals they have picked, which will then delay the
512 whole campaign. However, regarding scenario 1, where earthquakes occur at daytime, limited number

513 of injured inhabitants will be located at periphery areas of the community, leading to a lower demand
514 on the network, which helps to maintain a local equilibrium. In particular, when more CAVs have been
515 engaging in the campaign, the stagnancy associated with the post-shock transfer has been effectively
516 alleviated, throughout both the downtown and periphery areas. As shown in Fig. 4 (a), no delay is
517 observed until the moment when the majority of the injured inhabitants have been admitted to the
518 hospital system already.

519 However, as shown in Section 4.2, the advantage of CAVs can be substantially reduced, in the case
520 with the majority of the injured in the periphery, which is the setup of scenario 3. The mismatch between
521 the supply and demand in such a scenario, **with regard to the hospital system**, will lead to longer-distance
522 travel for many injured inhabitants, who need to reach those hospitals in the downtown. In particular,
523 due to the sparsity of road segments in the periphery and the limited river crossing, the dynamic route
524 programming of CAVs would sometimes bring about the detour (to circumvent those congested
525 segments), which will, paradoxically, prolong the transfer. As shown in Fig. 5 (a), despite the shorter
526 GTTs regarding the whole campaign, those cases with the presences of CAVs are even trailing the
527 baseline, in the early stage of the transfer.

528 Compared to scenarios 1 and 3, transfer in scenarios 2 and 4 are significantly more sluggish, leading
529 to GTTs that are up to 4 times longer. As mentioned above, the uninformed choice of hospitals will cause
530 re-selection and re-transfer for a large number of agents, as a result of the absence of the real-time
531 information sharing in such two scenarios. When it comes to the real-world hazard events, the significant
532 re-transfer endeavor would contribute to the lack of coordination of the traffic flow across local road
533 networks, alongside other vehicles (e.g. driven by those who are not wounded by the hazard, but are
534 moving to other intact communities), which are not even modelled in this framework. It shall be
535 particularly highlighted that, such an uncoordinated traffic flow will have a cascading effect on the post-
536 shock transfer, in the sense that the long-lasting and pervasive congestion on several road segments
537 (especially those critical ones, for example, connecting those hospitals with functionality grade *I*) will
538 limit the contribution of CVAs, despite their route planning capabilities (as shown in both Figs. 4 and
539 5), and ultimately, increase the mortality and socio-economic losses under hazard events. Furthermore,
540 the other emergency responses endeavors (e.g. fire extinguishment, debris removal, and etc.) will also
541 be substantially hindered, and the resilience of the whole community will be thus reduced.

542 In summary, the agent-based model developed in this research has highlighted that uncoordinated
543 transfer on the system-level can be triggered by the lack of adaptivity on the individual level. On the
544 contrary, more rational decision regarding the hospital selection, owing to the access to the real-time
545 information of the local hospital system, can significantly streamline the citywide transfer throughout
546 public emergencies. Furthermore, behavior of those transfers can be further ameliorated through the
547 deployment of the fleet of CAVs, who are essentially able to maximize the usage of the real-time

548 connectivity of the local road network, through dynamic route planning. Therefore, in view of its
549 granularity, the proposed framework can serve as a viable tool for stakeholders and administrators of
550 future urban communities to develop appropriate emergency response strategies, while formulating risk
551 governance policies. Besides, given its inclusiveness, more complex behavior patterns of individuals
552 and other sociological factors can be also incorporated into such an ABM framework.

553 Notwithstanding the new insights generated and discussed above, it should be noted that, given the
554 burgeoning study into the self-driving vehicles (Badue et al. 2021), more research needs to be
555 conducted to model the nuanced responsive behavior of future CAVs under complex on-road
556 conditions, throughout public emergencies, whereby the developed framework in this paper can be
557 further tailored to future urban communities with intelligent road networks (Fu et al. 2021).

558 **5. Conclusions**

559 Throughout the past decades, urbanization has become an inexorable trend around the globe.
560 Accordingly, modern urban communities have served as the engine for wealth creation and technological
561 advance, in most of the nations (Bettencourt et al. 2017). Nevertheless, the advantage of booming urban
562 communities has often been found to be offset by the recurrent curses of various catastrophes (Glaeser
563 2011), especially, natural hazards. Against this backdrop, the public health resilience of those hazard-
564 impacted urban communities can be thus jeopardized, and it is thus strategically crucial to develop a
565 principled understanding on the post-hazard massive transfer across those communities, incorporating
566 aspects ranging from hazard scenarios, to the behavioral pattern of injured inhabitants, as well as the
567 topological configuration and operational dynamic of an array of critical infrastructure systems serving
568 them, throughout public emergencies.

569 Meanwhile, in light of the increasing penetration of artificial intelligence that is revolutionizing the
570 modus operandi of modern urban communities, deployment and participation of CAVs are also expected
571 to reshape those massive transfer campaigns. Compared to conventional vehicles, i.e. HDVs, CAVs are
572 capable of planning the travel route autonomously, by exploring the real-time functionality status of
573 local road network in the course of the transfer, which can be strategically crucial to the coordination
574 among individual vehicles engaging in those campaigns. Moreover, CAVs could also be particularly
575 conducive to the transfer of those hazard-injured inhabitants, as well as other vulnerable groups, who
576 are struggling to drive on their own. Nevertheless, research on the impact of the participation of CAVs
577 on large-scale, post-shock transfer has been merger, so far.

578 To fill in such a knowledge gap, as a bottom-up approach to complex and large-scale socio-economic
579 systems with interacting entities (Batty 2007, Sun et al. 2019), an ABM framework, where each injured
580 inhabitant is modeled as an independent agent, who can be transferred to local hospitals by either HDVs
581 or CVAs, has been developed in this study. To demonstrate its applicability, this framework is applied
582 to model the post-earthquake emergency transfer across the networked hospital system-road network-

583 community in Tangshan city, which is located in one of the most earthquake-prone regions of China.
584 Particularly, in such a case-study, the impact of the initial spatiotemporal distribution of earthquake-
585 initiated wounded inhabitants, the percentage of inhabitants (engaging in the transfer campaign)
586 transferred by CAVs, and the real-time information of the functionality status of the local hospital system
587 on the citywide transfer, has been investigated. A host of conclusions have been drawn from the outcome
588 of that study, as the following:

- 589 1. Owing to its granularity, the ABM framework proposed in this paper can deliver a nuanced
590 modelling on the city-scale transfer campaigns, with the participation of a fleet of CAVs;
- 591 2. The spatial distribution of earthquake-initiated wounded inhabitants is found to have a profound
592 impact on the behavior of the post-shock transfer. **Regarding** scenarios with earthquake at
593 nighttime, the mismatch between the supply and demand on the hospital functionality will render
594 the transfer campaign susceptible to disruptions;
- 595 3. The lack of real-time information regarding the hospital system functionality will substantially
596 complicate and prolong post-shock transfer campaigns, in view of the system-level incoordination,
597 as a result of the irrational hospital selection of a significant fraction of injured inhabitants;
- 598 4. The participation of large number of CAVs can significantly expedite the post-shock transfer. In
599 terms of earthquakes at daytime, a reduction of nearly 30% has been observed, regarding the gross
600 transfer time in the case of just 40% of CAVs. It can be thereby concluded that the deployment of
601 a fleet of CAVs, even with only a moderate size, can be strategically critical to the minimization
602 of mortality of **earthquake-impacted** urban communities. It is also noteworthy that, unlike HDVs,
603 the negative impact of panic and potentially irrational behavior of human beings (throughout
604 emergencies) upon post-shock transfers can be effectively curbed by CAVs. The cost-
605 effectiveness of the investment on that deployment of CAVs can be **thereby further increased**, for
606 future urban communities.

607 Meanwhile, it shall also be noted that the casualty of urban communities under hazardous events can be
608 profoundly impacted by an array of additional influential factors, e.g. the age, the underlying health
609 condition, and the household income of those injured inhabitants, which have not been modelled in this
610 study. Besides, as already highlighted by the case-study, apart from the local hospital system alone, the
611 post-shock transfer and rescue will also be reshaped by the real-time functionality of the road network,
612 the telecommunication system, as well as a host of other infrastructure systems embedded in the same
613 region, given the looped interdependence within modern urban communities (Kröger and Zio 2011,
614 Helbing 2013, Zhao and Sun 2021). By incorporating those factors into account, further research needs
615 to be conducted to develop a more adaptive, coordinated and targeted strategy of post-shock rapid
616 response, including emergency transfers, whereby the human, economic, and societal losses can be
617 minimized, following the inclusive ABM framework proposed in this paper.

618

619 Acknowledgements

620 The first author would like to acknowledge the financial support from China Scholarship Council (CSC),
621 under the Grant No. 202006090155.

622

623

624

625 Reference

- 626 1. Atkinson, G. M., and Boore, D. M. (1995). Ground-motion relations for eastern North America. *Bulletin of*
627 *the Seismological Society of America* 85(1):17-30.
- 628 2. Badue, C., Guidolini, R., Carneiro, R. V., and Azevedo, P. et al. (2021). Self-driving cars: A survey. *Expert*
629 *Systems with Applications* 165: 113816.
- 630 3. Batty, M. (2007). *Cities and complexity: Understanding cities with cellular automata, agent-based models,*
631 *and fractals*. Cambridge, Massachusetts, MIT Press, United States.
- 632 4. Bettencourt, L. M. A., Lobo, J., Helbing, D., Kuhnert, C., and West, G. B. (2007). Growth, innovation, scaling,
633 and the pace of life in cities. *Proceedings of the National Academy of Sciences* 104(17): 7301-7306.
- 634 5. Branston, D. (1976). Link capacity functions-Review. *Transportation Research* 10(4): 223-236.
- 635 6. Byun, J. E., and D'Ayala, D. (2022). Urban seismic resilience mapping: a transportation network in Istanbul,
636 Turkey. *Scientific Reports* 12(1): 8188.
- 637 7. Ceferino, L., Kiremidjian, A., and Deierlein, G. (2018). Probabilistic model for regional multiseverity casualty
638 estimation due to building damage following an earthquake. *ASCE-ASME Journal of Risk and Uncertainty in*
639 *Engineering Systems, Part A: Civil Engineering* 4(3): 04018023.
- 640 8. Ceferino, L., Mitrani-Reiser, J., Kiremidjian A., Deierlein, G., and Bambarén C. (2020). Effective plans for
641 hospital system response to earthquake emergencies. *Nature Communications* 11(1): 4325.
- 642 9. Cetin, N., Burri, A., and Nagel, K. (2003). A large-scale agent-based traffic micro simulation based on queue
643 model. *Proceedings of Swiss Transport Research Conference (STRC), Monte Verita, Switzerland*.
- 644 10. Chen, Y. X., Liu, M., and Wang, H. (2021). Aftershocks and background seismicity in Tangshan and the rest
645 of North China. *Journal of Geophysical Research: Solid Earth* 126(5): e2020JB021395.
- 646 11. Cimellaro, G. P., Ozzello, F., Vallero, A., Mahin, S., and Shao, B. (2017). Simulating earthquake evacuation
647 using human behavior models. *Earthquake engineering and structural dynamics* 46(6): 985-1002.
- 648 12. Cimellaro, G. P., Reinhorn, A. M., and Bruneau, M. (2011). Performance-based metamodel for healthcare
649 facilities. *Earthquake Engineering and Structural Dynamics* 40 (11): 1197-1217.
- 650 13. Civljak, R., Markotic, A., and Capak, K. (2020). Earthquake in the time of COVID-19: The story from Croatia
651 (CroVID-20). *Journal of Global Health* 10(1): 010349.
- 652 14. Coburn, A. W., Spence, R. J., and Pomonis, A. (1992). Factors determining human casualty levels in
653 earthquakes: mortality prediction in building collapse. *The proceedings of the 1st international forum on*
654 *earthquake related casualties, Madrid, Spain*.
- 655 15. Del Papa, J., Vittorini, P., D'Aloisio, F., Muselli, M., Giuliani, A. R., Mascitelli, A., and Fabiani, L. (2019).
656 Retrospective Analysis of Injuries and Hospitalizations of Patients Following the 2009 Earthquake of L'Aquila
657 City. *International journal of environmental research and public health* 16(10): 1675.
- 658 16. Dijkstra, E. W. (1959). A note on two problems in connexion with graphs. *Numerische Mathematik* 1: 269-
659 271.
- 660 17. Fagnant, D. J., and Kockelman, K. (2015). Preparing a nation for autonomous vehicles: Opportunities, barriers
661 and policy recommendations. *Transportation Research Part A: Policy and Practice* 77: 167-181.
- 662 18. Feng, K. R., Li, Q. W., and Ellingwood, B. R. (2020). Post-earthquake modelling of transportation networks
663 using an agent-based model. *Structure and Infrastructure Engineering* 16(11): 1578-1592.
- 664 19. Fu, X., Nie, Q. F., Liu, J., Khattak, A., Hainen, A., and Nambisan, S. (2021). Constructing spatiotemporal
665 driving volatility profiles for connected and automated vehicles in existing highway networks. *Journal of*
666 *Intelligent Transportation Systems*, Accepted.
- 667 20. Glaeser, E. (2011). Cities, productivity, and quality of life. *Science* 333(6042): 592-594.
- 668 21. Hara, Y., and Kuwahara, M. (2015). Traffic monitoring immediately after a major natural disaster as revealed
669 by probe data-A case in Ishinomaki after the Great East Japan Earthquake. *Transportation Research Part A:*
670 *Policy and Practice* 75:1-15.

- 671 22. Hart, P. E., Nilsson, N. J., and Raphael, B. (1968). A formal basis for the heuristic determination of minimum
672 cost paths. *IEEE Transactions on Systems Science and Cybernetics* 4(2): 100-107.
- 673 23. Hassan, E. M., and Mahmoud, H. (2020). An integrated socio-technical approach for post-earthquake recovery
674 of interdependent healthcare system. *Reliability Engineering and System Safety* 201: 106953.
- 675 24. He, C. Y., Huang, Q. X., Dou, Y. Y., Tu, W., and Liu, J. F. (2016). The population in China's earthquake-
676 prone areas has increased by over 32 million along with rapid urbanization. *Environmental Research Letters*
677 11(7): 074028.
- 678 25. Helbing, D., Farkas, I., and Vicsek, T. (2000). Simulating dynamical features of escape panic. *Nature*
679 407(6803): 487-490.
- 680 26. Helbing, D., and Mazloumian, A. (2009). Operation regimes and slower-is-faster effect in the control of traffic
681 intersections. *European Physical Journal B* 70(2): 257-274.
- 682 27. Helbing, D. (2013). Globally networked risks and how to respond. *Nature* 497(7447): 51-59.
- 683 28. Jacques, C. C., McIntosh, J., Giovinazzi, S., Kirsch, T. D., Wilson, T., and Mitrani-Reiser, J. (2014). Resilience
684 of the Canterbury hospital system to the 2011 Christchurch earthquake. *Earthquake Spectra* 30 (1): 533-554.
- 685 29. Jaiswal, K., Wald, D., and D'Ayala, D. (2011). Developing empirical collapse fragility functions for global
686 building types. *Earthquake Spectra* 27(3): 775-795.
- 687 30. Krishnamurthy, V., Kwasinski, A., and Duenas-Osorio, L. (2016). Comparison of power and
688 telecommunications dependencies and interdependencies in the 2011 Tohoku and 2010 Maule Earthquakes.
689 *Journal of Infrastructure Systems* 22(3): 04016013.
- 690 31. Kröger, W., and Zio, E. (2011). *Vulnerable Systems*. London: Springer.
- 691 32. Kwiatkowski, R., and Lipson, H. (2019). Task-agnostic self-modeling machines. *Science Robotics* 4(26):
692 eaau9354.
- 693 33. Lin, C. C. J., Hung, H. H., Liu, K. Y., and Chai, J. F. (2010). Reconnaissance observation on bridge damage
694 caused by the 2008 Wenchuan (China) earthquake. *Earthquake spectra* 26(4): 1057-1083.
- 695 34. Li, X. M., Huang, J. S., and Zhang, H. (2008). An analysis of hospital preparedness capacity for public health
696 emergency in four regions of China: Beijing, Shandong, Guangxi, and Hainan. *BMC Public Health* 8: 319.
- 697 35. Lipson, H., and Kurman, M. (2022). *Driverless at last: Cars, artificial intelligence, and you*. Cambridge,
698 Massachusetts, MIT Press, United States.
- 699 36. Li, Q. P., Zhong, S., Fang, Z. X., Liu, L., Tu, W., and Chen, B. (2020). Optimizing mixed pedestrian-vehicle
700 evacuation via adaptive network reconfiguration. *IEEE Transactions on Intelligent Transportation Systems*
701 21(3): 1023-1033.
- 702 37. Lomnitz, C., and Lomnitz, L. (1978). Tangshan 1976: a case history in earthquake prediction. *Nature*
703 271(5641): 109-111.
- 704 38. Miller, M., and Baker, J. W. (2016). Coupling mode-destination accessibility with seismic risk assessment to
705 identify at-risk communities. *Reliability Engineering and System Safety* 147: 60-71.
- 706 39. Ouyang, M., Duenas-Osorio, L., and Min, X. (2012). A three-stage resilience analysis framework for urban
707 infrastructure systems. *Structural Safety* 36-37: 23-31.
- 708 40. Ouyang, M. (2014). Review on modeling and simulation of interdependent critical infrastructure systems.
709 *Reliability Engineering and System Safety* 121: 43-60.
- 710 41. Russell, S., and Norvig, P. (2021). *Artificial Intelligence: A Modern Approach (Fourth Edition)*. Pearson.
- 711 42. Schrittwieser, J., Antonoglou, I., Hubert, T., and Simonyan, K. et al. (2020). Mastering Atari, Go, chess and
712 shogi by planning with a learned model. *Nature* 588(7839): 604-+.
- 713 43. Stupazzini, M., Infantino, M., Allmann, A., and Paolucci, R. (2021). Physics-based probabilistic seismic
714 hazard and loss assessment in large urban areas: A simplified application to Istanbul. *Earthquake Engineering*
715 *and Structural Dynamics* 50 (1): 99-115.
- 716 44. Sun L., Didier M., Dele E., and Stojadinovic, B. (2015). Probabilistic demand and supply resilience model for
717 electric power supply system under seismic hazard. *The proceedings of the 12th international conference on*
718 *applications of statistics and probability in civil engineering (ICASP12), Vancouver, Canada*.
- 719 45. Sun, L., D'Ayala, D., Fayjaloun, R., and Gehl, P. (2021). Agent-based model on resilience-oriented rapid
720 responses of road networks under seismic hazard. *Reliability Engineering and System Safety* 216: 108030.
- 721 46. Sun, L., Stojadinovic, B., and Sansavini, G. (2019). Agent-based recovery model for seismic resilience
722 evaluation of electrified communities. *Risk Analysis* 7(39): 1597-1614.
- 723 47. Toma-Danila, D., Tiganescu, A., D'Ayala, D., Armas, I., and Sun, L. (2022). Time-dependent framework for
724 analyzing emergency intervention travel times and risk implications due to earthquakes: Bucharest case study.
725 *Frontiers in Earth Science* 10: 834052.
- 726 48. United Nations (2018). 2018 revision of world urbanization prospects.
727 <https://www.un.org/development/desa/publications/2018-revision-of-world-urbanization-prospects.html>

728 49. Van den Berg, V. A. C., and Verhoef, E. T. (2016). Autonomous cars and dynamic bottleneck congestion: The
729 effects on capacity, value of time and preference heterogeneity. *Transportation Research Part B:
730 Methodological* 94: 43-60.

731 50. Wang, Y., Kyriakidis, M., and Dang, V. N. (2021). Incorporating human factors in emergency evacuation-An
732 overview of behavioral factors and models. *International Journal of Disaster Risk Reduction* 60: 102254.

733 51. Wang, H. Z., Mostafizi, A., Cramer, L. A., Cox, D., and Park, H. (2016). An agent-based model of a multimodal
734 near-field tsunami evacuation: Decision-making and life safety. *Transportation Research Part C: Emerging
735 Technologies* 64: 86-100.

736 52. World Health Organization. (2022). WHO Coronavirus (Covid-19) dashboard. <https://covid19.who.int/>

737 53. Wu, J. H., Weng, W. G., and Ni, S. J. (2010). Urban emergency evacuation plans based on GIS and multi-
738 agent systems. *Journal of Tsinghua University* 50(8): 1168-1172 (in Chinese).

739 54. Yan, J. Q., Chen X. Z., and Sun, B. T. (2021). Review of estimation methods and systems used to predict
740 earthquake casualties. *Engineering Mechanics* 38(12): 1-16 (in Chinese).

741 55. Yavari, S., Chang, S. E., and Elwood, K. J. (2010). Modeling post-earthquake functionality of regional health
742 care facilities. *Earthquake Spectra* 26(3): 869-892.

743 56. Zhai, C., Yu, P., and Wen, W. (2021). A physical-organizational method for the functionality assessment of a
744 hospital subjected to earthquakes. *Journal of Earthquake Engineering*, Accepted.

745 57. Zhao, T., and Sun, L. (2021). Seismic resilience assessment of critical infrastructure-community systems
746 considering looped interdependences. *International Journal of Disaster Risk Reduction* 59: 102246.

747 58. Zhang, Y., Liu, L., Lu, Z., Wang, L., and Wen, X. (2020). Robust autonomous intersection control approach
748 for connected autonomous vehicles. *IEEE Access* 8: 124486-124502.

749
750
751
752
753
754
755
756